Dynamics of short pulses and phase matched second harmonic generation in negative index materials

Michael Scalora, Giuseppe D'Aguanno, Mark Bloemer

Charles M. Bowden Research Center, AMSRD-AMR-WS-ST, Research, Development, and Engineering Center, Redstone Arsenal, AL 35898-5000
michael.scalora@us.army.mil

Marco Centini

INFM at Dipartimento di Energetica, Universita di Roma 'La Sapienza', Via A. Scarpa 16, 00161 Roma, Italy

Domenico de Ceglia

Dipartimento di Elettrotecnica ed Elettronica, Politecnico di Bari, Via Orabona 4, 70124 Bari, Italy

Nadia Mattiucci

Time Domain Corporation, Cummings Research Park 7057 Old Madison Pike Huntsville, Alabama 35806, USA and Charles M. Bowden Research Center, AMSRD-AMR-WS-ST, Research, Development, and Engineering Center, Redstone Arsenal, AL 35898-5000

Yuri S. Kivshar

Nonlinear Physics Centre, Research School of Physical Sciences and Engineering, Australian National University, Canberra ACT 0200, Australia

Abstract: We study pulsed second harmonic generation in metamaterials under conditions of significant absorption. Tuning the pump in the negative index range, a second harmonic signal is generated in the positive index region, such that the respective indices of refraction have the same magnitudes but opposite signs. This insures that a forward-propagating pump is exactly phase matched to the backward-propagating second harmonic signal. Using peak intensities of ~500 MW/cm^2, assuming $\chi^{(2)}$~80pm/V, we predict conversion efficiencies of 12% and 0.2% for attenuation lengths of 50 and 5μm, respectively.

OCIS codes: (999.9999) Negative index materials; **(**190.2620) Frequency conversion; (260.2110) Electromagnetic theory

References and links

1. V.G. Veselago, "Electrodynamics of substances with simultaneously negative electrical and magnetic permeabilities," *Sov. Phys. USPEKHI* **10**, 509 (1968).
2. J.B. Pendry, "Negative refraction makes a perfect lens," Phys. Rev. Lett. **85,** 3966 (2000).
3. E. Yablonovitch, "Inhibited spontaneous emission in solid-state physics and electronics," Phys. Rev. Lett. **58**, 2059 (1987).
4. S. John, "Strong localization of photons in certain disordered dielectric superlattices," Phys. Rev. Lett. **58**, 2486 (1987).
5. Focus issue on: Negative Refraction and Metamaterials, Opt. Express **11**, .639-760 (2003).
6. Focus issue on: Metamaterials, J. Opt. Soc. Am. B **23**, 386-583 (2006).
7. M. Lapine, M. Gorkunov, and K. H. Ringhofer, "Nonlinearity of a metamaterial arising from diode insertions into resonant conductive elements," Phys. Rev. E **67**, 065601 (2003).

#69149 - $15.00 USD Received 21 March 2006; revised 8 May 2006; accepted 10 May 2006

8. V.M. Agranovich, Y.R. Shen, R. H. Baughman, and A. A. Zakhidov, "Linear and nonlinear wave propagation in negative index metamaterials," Phys. Rev. B **69**, 165112 (2004).
9. I.V. Shadrivov, A.A. Zharov, Y.S. Kivshar, "Second harmonic generation in nonlinear left-handed materials," J. Opt. Soc. Am. B **23**, 529 (2006).
10. A.K. Popov, V.V. Slabko, and V.M. Shalaev, "Second harmonic generation in left-handed materials," Las. Phys. Lett., published online February 2006.
11. M.V. Gorkunov, I.V. Shradivov, Y.S. Kivshar, "Enhanced parametric processes in binary metamaterials," Appl. Phys. Lett. **88**, 071912 (2006).
12. Jensen Li, Lei Zhou, C.T. Chan, and P. Sheng, "Photonic band gap from a stack of positive and negative index materials," Phys. Rev. Lett. **90**, 083901, (2003).
13. G. D'Aguanno, N. Mattiucci, M. J. Bloemer, and M. Scalora, "Large enhancement of second harmonic generation near the zero-n gap of a negative index Bragg grating," Phys. Rev. E **73**, 036603 (2006).
14. N. Mattiucci, G. D'Aguanno, M. J. Bloemer, and M. Scalora, "Second harmonic generation form a positive-negative index material heterostructure," Phys. Rev E **72**, 066612 (2005).
15. R.A. Shelby, D.R. Smith, and S. Schultz, "Experimental verification of a negative index of refraction," *Science **292***, 77 (2001); C. G. Parazzoli, R.B. Greegor, K. Li, B.E.C. Koltenbah, M. Tanielian, "Experimental verification and simulation of negative index of refraction using Snell's law," Phys. Rev. Lett. **90**, 107401 (2003).
16. M. Scalora, G. D'Aguanno, N. Mattiucci, M.J. Bloemer, J.W. Haus, A.M. Zheltikov, "Negative refraction of ultrashort electromagnetic pulses," Appl. Phys. B **81**, 393 (2005).
17. M. Scalora, M. Syrchin, N. Akozbek, E.Y. Poliakov, G. D'Aguanno, N. Mattiucci, M.J. Bloemer, A.M. Zheltikov, "Generalized nonlinear Schrodinger equation for dispersive susceptibility and permeability: applications to negative index materials," Phys. Rev. Lett. **95**, 013902 (2005).
18. M. Scalora, G. D'Aguanno, N. Mattiucci, N. Akozbek, M. J. Bloemer, M. Centini, C. Sibilia, M. Bertolotti, "Pulse propagation, dispersion, and energy in negative index materials," Phys. Rev. E **72**, 066601 (2005).
19. A. Zharov, I.V. Shadrivov, Y.S. Kivshar, "Nonlinear properties of left-handed materials," Phys. Rev. Lett. **91**, 037401 (2003).
20. M. Centini, C. Sibilia, M. Scalora, G. D'Aguanno, M. Bertolotti, M. J. Bloemer, C. M. Bowden, and I. Nefedov, "Dispersive properties of finite, one-dimensional photonic band gap structures: applications to nonlinear quadratic interactions," Phys. Rev. E **60**, 4891 (1999).
21. M. Scalora, M.J. Bloemer, A.S. Manka, J.P. Dowling, C.M. Bowden, R. Viswanathan, J.W. Haus, "Pulsed second harmonic generation in nonlinear, one-dimensional, periodic structures," Phys. Rev. A **56**, 3166-75 (1997).
22. Y. Dumeige, P. Vidakovic, S. Sauvage, I. Sagnes, J. A. Levenson, C. Sibilia, M. Centini, G. D'Aguanno, M. Scalora, "Enhancement of second harmonic generation in one-dimensional semiconductor photonic band gap," Appl. Phys. Lett. **78**, 3021 (2001).
23. Y. Dumeige, I. Sagnes, P. Monnier, P. Vidakovic, I. Abram, C. Mériadec, J. A. Levenson, "Phase matched frequency doubling at photonic band edges: efficiency scaling as the fifth power of the length," Phys. Rev. Lett. **89**, 043901 (2002).

Recently, researchers have devoted a great deal of attention to negative index materials (NIM) [1,2], perhaps in a manner comparable in scope and magnitude to the interest that photonic band gap (PBG) materials have enjoyed for the last two decades [3,4]. Just as was the case for PBG materials, the study of NIMs appears to be characterized by a transitional stage during which workers have realized that the concept is quite appealing and powerful, probably because it calls for the re-evaluation of many of the same basic principles that have been developed for ordinary materials [5,6]. This gradual evolution of the field is accompanied by new opportunities and, as is often the case, by just as many challenges. A simple, representative example is nonlinear frequency conversion, second harmonic generation (SHG) in particular. The issue of SHG in bulk NIMs has been addressed by Lapine et al [7], who discussed the introduction of nonlinear elements in the microwave regime, and Agranovich and co-workers [8], and Shradivov et al [9], who have suggested that a forward propagating pump beam tuned in the negative index region, having a negative carrier wave vector, could be phase-matched to a backward-propagating second harmonic signal tuned in the positive index range and having positive wave vector. They showed that the efficiency of the process approaches 100% in the absence of absorption. Popov and co-workers [10] have also studied steady-state SHG in the context of bulk materials, and found that the Manley-Rowe relations can be unusual when compared to ordinary PIMs, due to the phase matching

#69149 - $15.00 USD Received 21 March 2006; revised 8 May 2006; accepted 10 May 2006

that occurs between counter-propagating beams. Also recently, Gorkunov at al have proposed the use of a doubly resonant system to induce perfect phase matching conditions, and order of magnitude enhancement of SHG [11].

SHG in NIMs has also been studied in cavity environments. It has been pointed out that SHG can occur for standard, centro-symmetric materials near the zero-n gap [12] of a Bragg grating made of alternating NIM/PIM layers [13]. It turns out that a combination of field localization and coherent oscillations of the nonlinear dipoles located at the structure's interfaces leads to conversion efficiencies at least an order of magnitude larger than those achievable in the same length of a nonlinear, phase-matched, bulk material. In a related development, coupled cavities composed of nonlinear PIMs and linear NIMs [14] also display advantages over more conventional cavities because the NIM materials make better mirrors, leading to improved field localization effects and enhanced emission.

The overarching theme that characterizes all the works cited above is that SHG is efficient only if absorption inside the NIM is negligible. In fact, all linear and nonlinear theoretical approaches used to model NIMs have relied heavily on the assumption that absorption should be avoided. Although this constraint may not be crucial in cavity surroundings if NIM layers are relatively thin, the issue becomes critical in bulk environments. Naturally, this is a severe restriction that can raise serious questions in the minds of arbiters and ordinary readers alike, and may also lead one to question whether any proposed NIM-related phenomenon is observable in a bulk setting. Any predictions must in fact be ultimately reconciled with the fact that experimental observations [15] strongly suggest that incident waves are significantly attenuated in NIMs. For this reason, in this paper we focus on the proposed phase-matched scheme for backward second harmonic generation, similar to that discussed in references [8,9], and show that the process remains efficient even when absorption plays a significant role. Specifically, using the Drude model, the integration of Maxwell's equations in the time domain reveals that a medium having the following, generic characteristics: (i) a $\chi^{(2)}$ ~ 80pm/V; (ii) pumped with pulses at least 2.5ps in duration, with peak intensities ~500MW/cm^2; is still capable of generating a backward-propagating (reflected) SH signal at a remarkable ~12% conversion efficiency rate even though the pump attenuation depth is roughly 50μm, and an equally impressive ~0.2% conversion rate for attenuation depths of 5μm.

We begin by writing nonlinear, second order polarization and magnetization as follows:

$$\mathbf{P}_{NL} = \chi_P^{(2)} \mathbf{E} \bullet \mathbf{E}; \qquad \mathbf{M}_{NL} = \chi_M^{(2)} \mathbf{H} \bullet \mathbf{H}, \tag{1}$$

where $\chi_P^{(2)}$ and $\chi_M^{(2)}$ are the electric and magnetic nonlinear coefficients, respectively. Assuming linearly polarized fields of the type:

$$\begin{aligned} \mathbf{E} &= \hat{\mathbf{x}}\left(\mathcal{E}_\omega(z,t) e^{i(kz-\omega_0 t)} + c.c + \mathcal{E}_{2\omega}(z,t) e^{2i(kz-\omega_0 t)} + c.c \right) \\ \mathbf{H} &= \hat{\mathbf{y}}\left(\mathcal{H}_\omega(z,t) e^{i(kz-\omega_0 t)} + c.c + \mathcal{H}_{2\omega}(z,t) e^{2i(kz-\omega_0 t)} + c.c \right) \end{aligned}, \tag{2}$$

the nonlinear polarization and magnetization may be written as:

$$\begin{aligned} \mathbf{P}_{NL} &= \hat{\mathbf{x}}\left(\mathcal{P}_\omega(z,t) e^{i(kz-\omega_0 t)} + c.c + \mathcal{P}_{2\omega}(z,t) e^{2i(kz-\omega_0 t)} + c.c \right) \\ \mathbf{M}_{NL} &= \hat{\mathbf{y}}\left(\mathcal{M}_\omega(z,t) e^{i(kz-\omega_0 t)} + c.c + \mathcal{M}_{2\omega}(z,t) e^{2i(kz-\omega_0 t)} + c.c \right) \end{aligned}, \tag{3}$$

where $\mathcal{P}_\omega(z,t) = 2\chi_P^{(2)} \mathcal{E}_\omega^* \mathcal{E}_{2\omega}$, $\mathcal{P}_{2\omega}(z,t) = \chi_P^{(2)} \mathcal{E}_\omega^2$ $\mathcal{M}_\omega(z,t) = 2\chi_M^{(2)} \mathcal{H}_\omega^* \mathcal{H}_{2\omega}$, and $\mathcal{M}_{2\omega}(z,t) = \chi_M^{(2)} \mathcal{H}_\omega^2$. The inclusion of linear dispersion is straight forward [16-18], and

#69149 - $15.00 USD Received 21 March 2006; revised 8 May 2006; accepted 10 May 2006

Maxwell's equations then take the following form:

$$\alpha_{\tilde{\omega}}\frac{\partial \mathcal{E}_{\tilde{\omega}}}{\partial \tau}+i\frac{\alpha'_{\tilde{\omega}}}{4\pi}\frac{\partial^2 \mathcal{E}_{\tilde{\omega}}}{\partial \tau^2}-\frac{\alpha''_{\tilde{\omega}}}{24\pi^2}\frac{\partial^3 \mathcal{E}_{\tilde{\omega}}}{\partial \tau^3}+\ldots=i\beta\left(\varepsilon_{\tilde{\omega},\xi}\mathcal{E}_{\tilde{\omega}}-\mathcal{H}_{\tilde{\omega}}\right)-\frac{\partial \mathcal{H}_{\tilde{\omega}}}{\partial \xi}+4\pi\left(i\beta\mathcal{P}_{\tilde{\omega}}-\frac{\partial \mathcal{P}_{\tilde{\omega}}}{\partial \tau}\right)$$

$$\gamma_{\tilde{\omega}}\frac{\partial H_{\tilde{\omega}}}{\partial \tau}+i\frac{\gamma'_{\tilde{\omega}}}{4\pi}\frac{\partial^2 \mathcal{H}_{\tilde{\omega}}}{\partial \tau^2}-\frac{\gamma''_{\tilde{\omega}}}{24\pi^2}\frac{\partial^3 \mathcal{H}_{\tilde{\omega}}}{\partial \tau^3}+\ldots=i\beta\left(\mu_{\tilde{\omega},\xi}\mathcal{H}_{\tilde{\omega}}-\mathcal{E}_{\tilde{\omega}}\right)-\frac{\partial \mathcal{E}_{\tilde{\omega}}}{\partial \xi}+4\pi\left(i\beta\mathcal{M}_{\tilde{\omega}}-\frac{\partial \mathcal{M}_{\tilde{\omega}}}{\partial \tau}\right)$$

$$\alpha_{2\tilde{\omega}}\frac{\partial \mathcal{E}_{2\tilde{\omega}}}{\partial \tau}+i\frac{\alpha'_{2\tilde{\omega}}}{4\pi}\frac{\partial^2 \mathcal{E}_{2\tilde{\omega}}}{\partial \tau^2}-\frac{\alpha''_{2\tilde{\omega}}}{24\pi^2}\frac{\partial^3 \mathcal{E}_{2\tilde{\omega}}}{\partial \tau^3}\ldots=2i\beta\left(\varepsilon_{2\tilde{\omega},\xi}\mathcal{E}_{2\tilde{\omega}}-\mathcal{H}_{2\tilde{\omega}}\right)-\frac{\partial \mathcal{H}_{2\tilde{\omega}}}{\partial \xi}+4\pi\left(i2\beta\mathcal{P}_{2\tilde{\omega}}-\frac{\partial \mathcal{P}_{2\tilde{\omega}}}{\partial \tau}\right) \quad (4)$$

$$\gamma_{2\tilde{\omega}}\frac{\partial H_{2\tilde{\omega}}}{\partial \tau}+i\frac{\gamma'_{2\tilde{\omega}}}{4\pi}\frac{\partial^2 \mathcal{H}_{2\tilde{\omega}}}{\partial \tau^2}-\frac{\gamma''_{2\tilde{\omega}}}{24\pi^2}\frac{\partial^3 \mathcal{H}_{2\tilde{\omega}}}{\partial \tau^3}\ldots=2i\beta\left(\mu_{2\tilde{\omega},\xi}\mathcal{H}_{2\tilde{\omega}}-\mathcal{E}_{2\tilde{\omega}}\right)-\frac{\partial \mathcal{E}_{2\tilde{\omega}}}{\partial \xi}+4\pi\left(i2\beta\mathcal{M}_{2\tilde{\omega}}-\frac{\partial \mathcal{M}_{2\tilde{\omega}}}{\partial \tau}\right)$$

where the temporal derivatives arise from the linear dispersion of the medium, $\alpha_{\tilde{\omega}}=\frac{\partial[\tilde{\omega}\varepsilon(\xi)]}{\partial\tilde{\omega}}|_{\omega_0}$, $\alpha'_{\tilde{\omega}}=\frac{\partial^2[\tilde{\omega}\varepsilon(\xi)]}{\partial\tilde{\omega}^2}|_{\omega_0}$, $\gamma_{\tilde{\omega}}=\frac{\partial[\tilde{\omega}\mu(\xi)]}{\partial\tilde{\omega}}|_{\omega_0}$, $\gamma'_{\tilde{\omega}}=\frac{\partial^2[\tilde{\omega}\mu(\xi)]}{\partial\tilde{\omega}^2}|_{\omega_0}$, and so on, and both ε and μ are complex functions of frequency (allowing for causal material dispersion) and of the spatial coordinate (allowing for spatial, material discontinuities). We have chosen λ_r=1μm as the reference wavelength, and have adopted the following scaling: $\xi=z/\lambda_r$ is the scaled longitudinal coordinate, $\tau=ct/\lambda_r$ is the time in units of the optical cycle, $\beta=2\pi\tilde{\omega}$ is the scaled wave vector, and $\tilde{\omega}=\omega/\omega_r$ is the scaled frequency. Although they contain no approximations other than the assumption that the medium is isotropic, under most circumstances Eqs.(4) may be simplified. For instance, in ordinary dielectric materials the dispersion length (associated with the second order temporal derivative on the left hand sides of Eqs.(4)) varies from a few millimeters for few-cycle pulses, to a few meters for pulses several tens or a few hundred wave cycles in duration. NIMs, however, are more dispersive than ordinary materials, as described by either a Drude or a Lorentz model near a resonance condition. Nevertheless, typical dispersion lengths in regions of interest range from several hundred to several thousand wave cycles, depending on incident pulse width. In any case, the typical absorption length that we consider, which varies from 5μm to approximately 50μm, may be several orders of magnitude smaller than higher order dispersion lengths. This fact by itself obviates the need for the inclusion of higher order terms beyond the first order temporal derivative, which affects the group velocity of the pulse and should be preserved. As a result, Eqs.(4) may be simplified to read:

#69149 - $15.00 USD Received 21 March 2006; revised 8 May 2006; accepted 10 May 2006

$$\alpha_{\tilde{\omega}}\frac{\partial \mathcal{E}_{\tilde{\omega}}}{\partial \tau}\approx i\beta\left(\varepsilon_{\tilde{\omega},\xi}\mathcal{E}_{\tilde{\omega}}-\mathcal{H}_{\tilde{\omega}}\right)-\frac{\partial \mathcal{H}_{\tilde{\omega}}}{\partial \xi}+4\pi\left(i\beta\mathcal{P}_{\tilde{\omega}}-\frac{\partial \mathcal{P}_{\tilde{\omega}}}{\partial \tau}\right)$$

$$\gamma_{\tilde{\omega}}\frac{\partial H_{\tilde{\omega}}}{\partial \tau}\approx i\beta\left(\mu_{\tilde{\omega},\xi}\mathcal{H}_{\tilde{\omega}}-\mathcal{E}_{\tilde{\omega}}\right)-\frac{\partial \mathcal{E}_{\tilde{\omega}}}{\partial \xi}+4\pi\left(i\beta\mathcal{M}_{\tilde{\omega}}-\frac{\partial \mathcal{M}_{\tilde{\omega}}}{\partial \tau}\right) \quad . \quad (5)$$

$$\alpha_{2\tilde{\omega}}\frac{\partial \mathcal{E}_{2\tilde{\omega}}}{\partial \tau}\approx 2i\beta\left(\varepsilon_{2\tilde{\omega},\xi}\mathcal{E}_{2\tilde{\omega}}-\mathcal{H}_{2\tilde{\omega}}\right)-\frac{\partial \mathcal{H}_{2\tilde{\omega}}}{\partial \xi}+4\pi\left(i2\beta\mathcal{P}_{2\tilde{\omega}}-\frac{\partial \mathcal{P}_{2\tilde{\omega}}}{\partial \tau}\right)$$

$$\gamma_{2\tilde{\omega}}\frac{\partial H_{2\tilde{\omega}}}{\partial \tau}\approx 2i\beta\left(\mu_{2\tilde{\omega},\xi}\mathcal{H}_{2\tilde{\omega}}-\mathcal{E}_{2\tilde{\omega}}\right)-\frac{\partial \mathcal{E}_{2\tilde{\omega}}}{\partial \xi}+4\pi\left(i2\beta\mathcal{M}_{2\tilde{\omega}}-\frac{\partial \mathcal{M}_{2\tilde{\omega}}}{\partial \tau}\right)$$

An inspection of both Eqs.(4) and (5) suggests that they are symmetric with respect to the introduction of either a nonlinear polarization or magnetization. Therefore, one could just as easily treat a magnetic nonlinearity [19], and obtain qualitatively similar results. Moreover, while we do not dwell on the precise origin of the nonlinearity, one can reasonably assume that the nonlinearity resides in the nonlinear dipoles, and/or that the dipoles (both electric and magnetic) are embedded within a background medium that responds nonlinearly [19]. With these considerations in mind, we assume $\chi_M{}^{(2)}=0$, and present our results.

In Fig.(1) we show the typical Drude dispersion, assuming $\varepsilon(\tilde{\omega})=\mu(\tilde{\omega})=n(\tilde{\omega})=1-\frac{\left(\omega_p^2/\omega_r^2\right)}{\tilde{\omega}^2+i\tilde{\gamma}\tilde{\omega}}$, and taking $\omega_p^2/\omega_r^2=1$ (the plasma frequency corresponds to the reference frequency); the damping coefficient (also scaled by the reference frequency) is $\tilde{\gamma}=10^{-3}$. This choice results in an attenuation length of approximately 50μm, so that the intensity of the peak of the pulse drops to 1/e of its input value within that distance, and it is down to approximately 1% at 200 microns from the surface. One may compare this to the degree of absorption (i.e. imaginary part of the index) exhibited by GaAs at λ~890nm.

In the same figure we also report the general trend of the conversion efficiency as a function of normalized frequency (we do not scale it for simplicity), and we also identify pump and SH tuning ranges. To obtain the conversion efficiency curve shown we used incident pulses approximately 600fs in duration, or 200 wave cycles, and peak field values of ~10^4 Volts/m. We then calculated the total SH energy emitted in both directions, defined as $W_T(\tau)=\int_{-\infty}^{\infty}U(\xi,\tau)d\xi$, where the integrand represents the local, instantaneous, energy density, normalized by the initial pump energy. We estimate that the second order dispersion length, defined as $L_D^{(2)}\sim\frac{\tau_p^2}{|k''|}$, where τ_p is pulse duration, and $k''=\frac{\partial^2 k}{\partial\tilde{\omega}^2}$, ranges between $800\lambda_r$ for 20 wave cycle pulses, to about $6\times10^4\lambda_r$ for 200 wave cycle pulses. Therefore, we are well justified in taking the necessary steps to distill Eqs.(5) from Eqs.(4).

#69149 - $15.00 USD Received 21 March 2006; revised 8 May 2006; accepted 10 May 2006

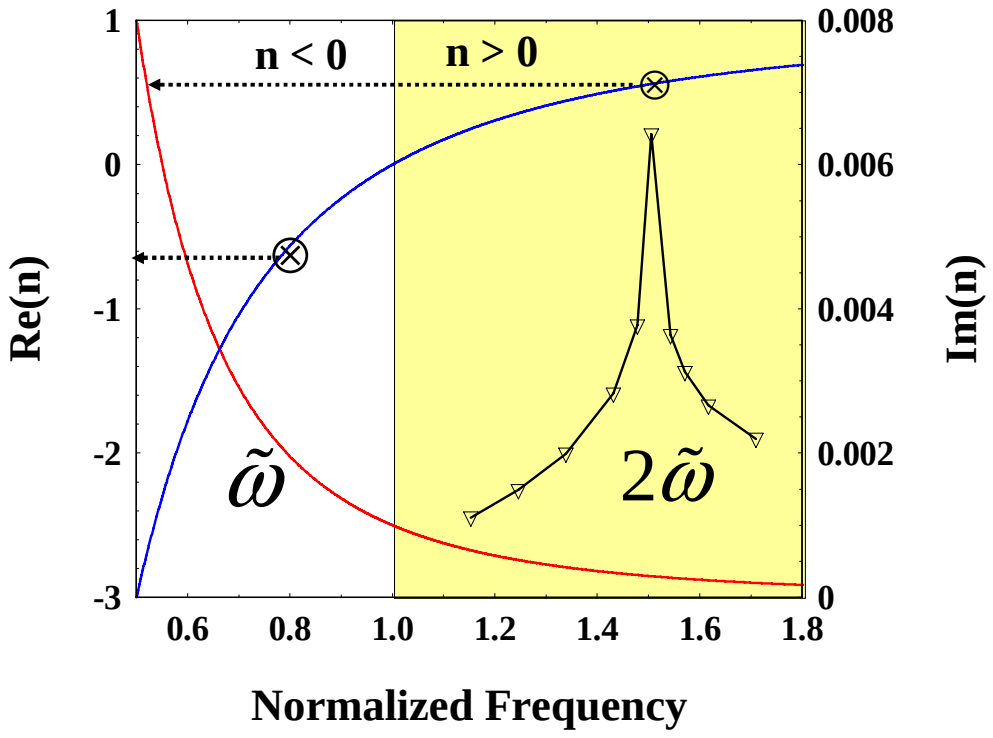

Fig. 1. Real (blue curve-left axis) and imaginary (red curve-right axis) parts of the index of refraction for the Drude model, with $\tilde{\gamma} = 10^{-3}$. The SH conversion efficiency, η, is also shown (solid black line with empty triangles-arbitrary scale). η sweeps across seven orders of magnitude from its minimum to its maximum, at the phase matching condition. $\tilde{\omega}$ and $2\tilde{\omega}$ indicate the tuning ranges of the fundamental and SH fields. The arrows point to the magnitudes of the indices of refraction at the fundamental and SH frequencies where the phase matching condition is approximately satisfied.

Figure 1 features the larger point we wish to make: at $\tilde{\omega} \approx 0.7905$, which corresponds to the highest SH efficiency at twice that frequency, the index of refraction calculated from the Drude dispersion is $n_{\tilde{\omega}} = -0.600278 + i0.002024$. At the second harmonic frequency, $2\tilde{\omega} \approx 1.581$, the index of refraction is positive, $n_{2\tilde{\omega}} = 0.599929 + i0.000253$. The phase matching condition between fundamental and SH pulses, which requires $\left(k_{2\omega} - 2k_{\omega}\right) = 0$, is nearly exactly satisfied for the backward generated SH pulse [8,9]. Neglecting the imaginary part, we have: $\left(k_{2\tilde{\omega}} - 2k_{\tilde{\omega}}\right) = 2\pi\left(-2\tilde{\omega}\,|\,n_{2\tilde{\omega}}\,| + 2\tilde{\omega}\,|\,n_{\tilde{\omega}}\,|\right) \sim 2\times10^{-3}$.

In Fig. 2 we show the typical scenario that unfolds as a 200 wave-cycle, 500MW/cm^2 incident pulse (corresponding to a field ~3x10^{7}V/m) crosses into a nonlinear NIM from vacuum. The pump is quickly attenuated, as a SH pulse is generated in the backward direction and rapidly exits the medium. The Drude dispersion reveals that the SH absorption length is approximately ten times larger compared to the pump absorption length, as can easily be deduced from the relative magnitudes of the imaginary part of the index.

#69149 - $15.00 USD
Received 21 March 2006; revised 8 May 2006; accepted 10 May 2006

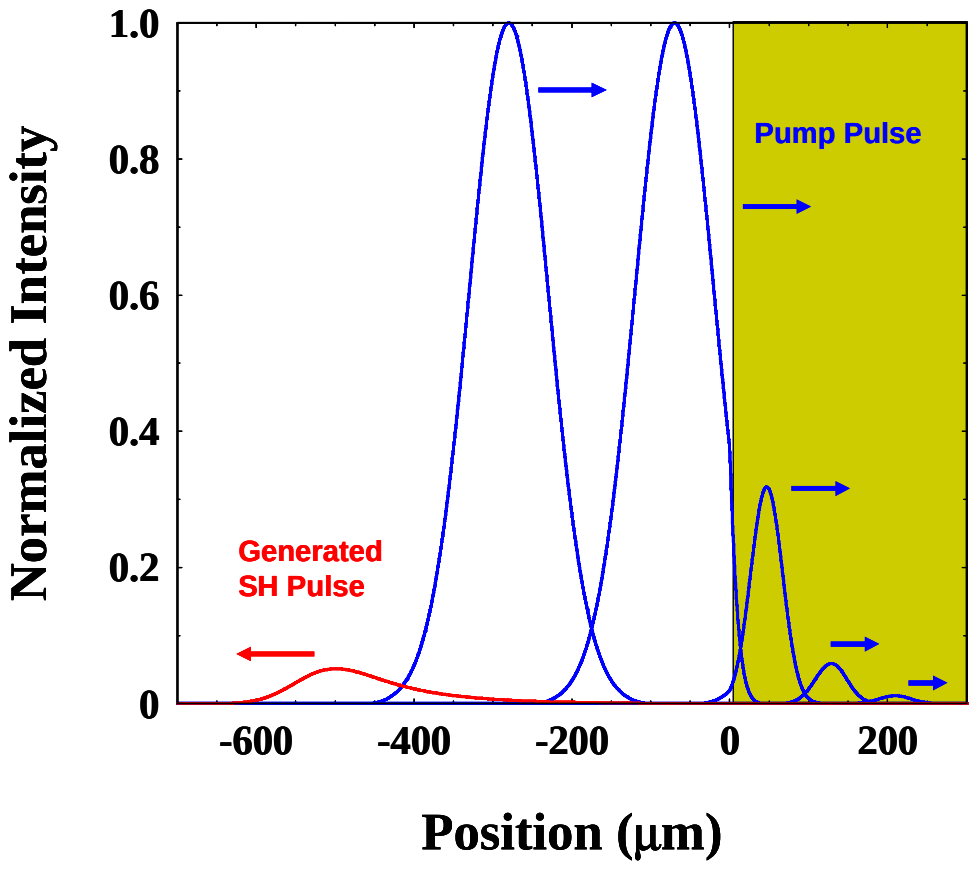

Fig. 2. A 600fs (200 wave cycles) pump (blue curve) is incident on a NIM (shaded region) from vacuum, and tuned to $\tilde{\omega}=0.7905$. The choice $\tilde{\gamma}=10^{-3}$ results in an attenuation depth of ~50μm. Most of the SH signal (red curve) is generated backward under nearly exact phase matching condition, at $2\tilde{\omega}=1.581$.

The study of pulsed dynamics reveals several noteworthy characteristics. For instance, in Fig. 3 we depict the conversion efficiency as a function of incident pulse duration, for two values of the damping coefficient. Given $\tilde{\gamma}=10^{-3}$, η_{SH} varies from ~2.5% for pulses 200fs in duration, to ~12% for pulses ~2.5ps long. On the same figure we also show the conversion efficiency for $\tilde{\gamma}=10^{-2}$. Changing $\tilde{\gamma}$ in this fashion leads to an order of magnitude increase in the imaginary part of the index, and reduces the attenuation depth down to 5μm, with marginal effects to the real part of the index. Nevertheless, the conversion efficiency still reaches ~0.2%. The figure also suggests that the efficiency improves by increasing pulse duration. This can be understood in terms of incident pulse bandwidth: as we increase pulse duration, more of the pulse comes into the phase matching condition, which is almost exactly satisfied at the carrier wavelength.

#69149 - $15.00 USD
Received 21 March 2006; revised 8 May 2006; accepted 10 May 2006

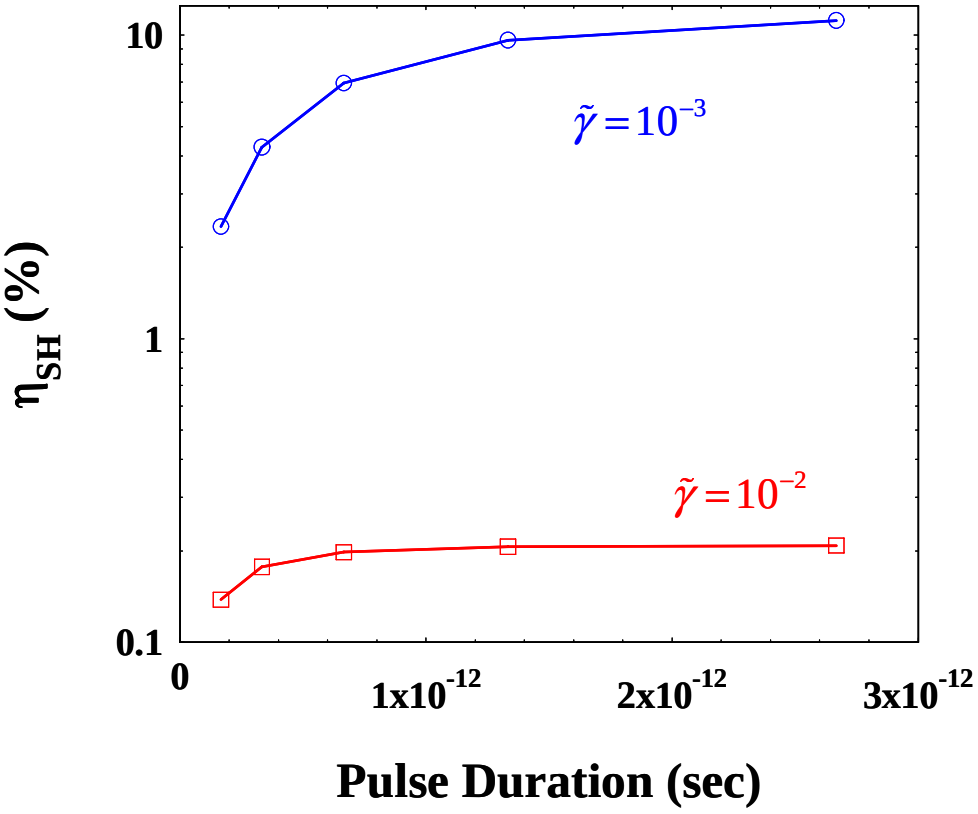

Fig. 3. SH conversion efficiency (%) as a function of incident pulse duration, for $\tilde{\gamma} = 10^{-3}$ and $\tilde{\gamma} = 10^{-2}$, assuming $\chi^{(2)}$~80pm/V and a peak intensity of ~500MW/cm^2. For $\tilde{\gamma} = 10^{-3}$, the attenuation depth is ~50μm. For $\tilde{\gamma} = 10^{-2}$, the attenuation depth is drastically reduced to ~5μm. Quasi-monochromatic pulses, i.e. pulse duration greater than 2.5ps, yield conversion efficiencies of ~12% and ~0.2%, respectively.

In Fig. 4 we show the Fourier decomposition of the incident and scattered pump fields. We have three major components: (i) the input wave packet; (ii) a transmitted component, having negative wave vector; and (iii) a low intensity, reflected component. Reflection is small (less then 1 part in 10^7), because we have assumed that $\varepsilon=\mu$, a restriction that can easily be removed.

In Fig. 5 we show the Fourier components of the SH signal. Here, too, we find three major components: (i) the one generated backward, that has already exited into free space, at twice the incident pump wave-vector; (ii) the phase matched component, traveling backward inside the medium toward the entrance interface, with wave vector almost precisely at twice the pump wave vector; (iii) a forward-moving, SH component, generated far from the phase matching condition, which is being absorbed away.

#69149 - $15.00 USD
Received 21 March 2006; revised 8 May 2006; accepted 10 May 2006

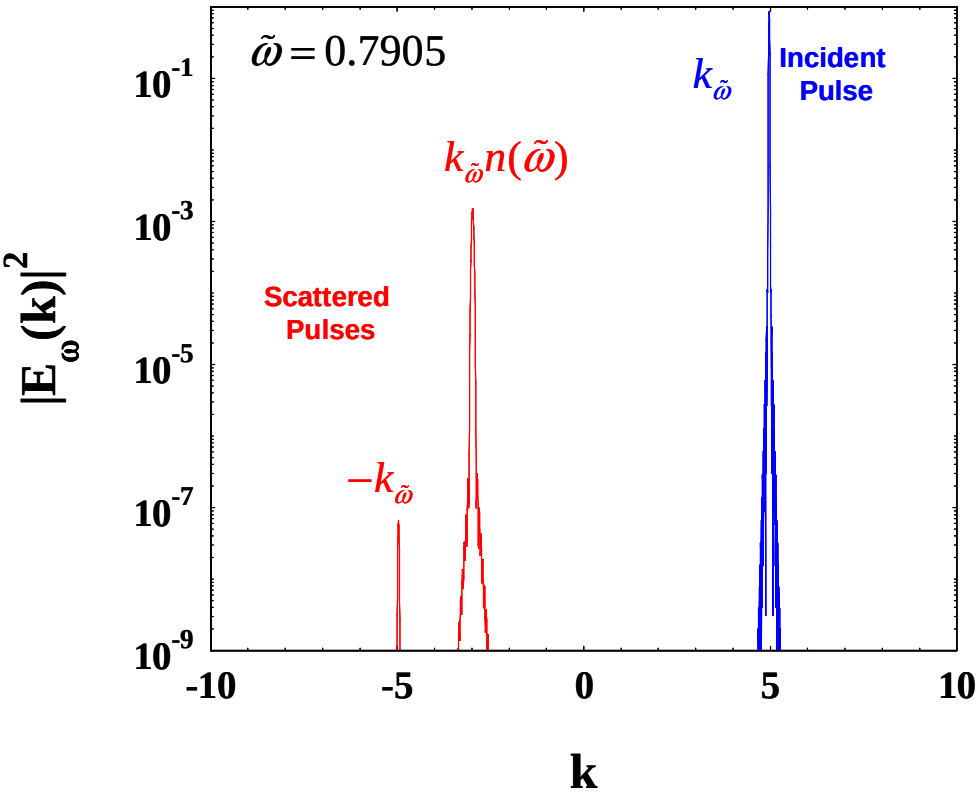

Fig. 4. Fourier decomposition of the incident ($k_{\tilde{\omega}}$) and scattered pump pulses. The wave number is dimensionless. The transmitted wave packet $(k_{\tilde{\omega}} n(\tilde{\omega}))$ is a superposition of negative wave vectors, even though the pulse propagates in the forward direction. There is a small reflected component propagating backward in free space ($-k_{\tilde{\omega}}$).

The conversion efficiencies that we report are large by any measure, considering the amount of absorption we have introduced. Even though the magnitude of the nonlinear coefficient may be somewhat large, all things being equal, i.e. $\chi^{(2)}$ and incident peak power, it would be possible to obtain similar conversion efficiencies if, in the absence of absorption, two conditions could be satisfied: (i) exact phase and (ii) group velocity matching. For comparison purposes, if a 200fs, 500MW/cm^2 pulse were incident on a semi-infinite, ideally matched medium having n~1.42, one obtains a conversion efficiency of η~10% after the peak of the pulse propagates ~45μm. In contrast, the introduction of an index mismatch due to normal material dispersion (we consider a typical index variation of ~6% between ω (n~1.42)and 2ω (n~1.52)), along with an appropriate group velocity mismatch ($V_g^{\tilde{\omega}} \sim c/1.57$; $V_g^{2\tilde{\omega}} \sim c/2.2$), reduces the conversion efficiency dramatically down to η~0.01%, with further decreases if absorption is added. We should note that a group velocity mismatch has a much less pronounced impact on conversion efficiency compared to an index mismatch, as expected, but it can make its impact felt, particularly for shorter pulses. However, it is not feasible to simultaneously have phase and group velocity matching in a bulk medium, as natural material dispersion generally does not allow it.

#69149 - $15.00 USD Received 21 March 2006; revised 8 May 2006; accepted 10 May 2006

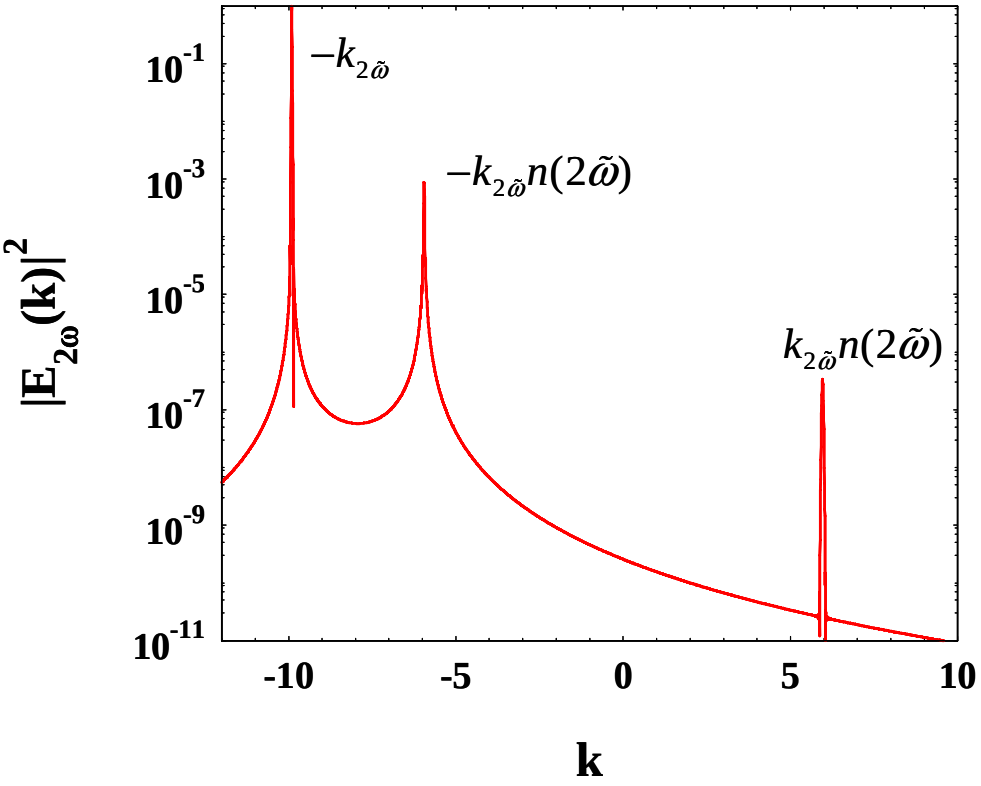

Fig. 5. Fourier decomposition of the generated SH field. The wave number is dimensionless, as in Fig. 4. The positive component identifies a mismatched signal propagating forward inside the medium ($k_{2\tilde{\omega}}n(2\tilde{\omega})$), that is eventually absorbed away. The negative components correspond to a signal that has already emerged in vacuum, and has twice the incident wave vector ($-k_{2\tilde{\omega}}$), and a signal traveling in the negative direction, inside the medium ($-k_{2\tilde{\omega}}n(2\tilde{\omega})$), that will eventually exit into the vacuum.

Indeed it is possible to have effective phase matching and achieve approximately similar group velocities for the fundamental and SH waves in photonic band gap structures, where geometrical dispersion can be used to compensate the naturally occurring material dispersion [20, 23]. Nevertheless, absorption usually has a detrimental effect that significantly reduces conversion efficiency under any circumstances where the beams co-propagate, including resonant conditions. In contrast, the unusual phase matching conditions that naturally occur in a NIM for counter-propagating waves also suffer the effects of absorption, but not to the same detrimental degree because the rapid decay of the pump along the positive direction is accompanied by an equally swift exponential increase of the SH signal toward the nearby entry surface. In addition to nearly exact phase matching conditions, the fields overlap for the entire duration of the pump pulse, and the impact of absorption is minimized.

#69149 - $15.00 USD Received 21 March 2006; revised 8 May 2006; accepted 10 May 2006

In conclusion, we have shown that second harmonic generation can occur in a NIM and be relatively efficient in the presence of significant absorption. Assuming a Drude dispersive model, we have shown that a phase matching condition established between counter-propagating fundamental and second harmonic waves helps boost conversion efficiencies up to 12% for the reflected SH component when the attenuation depth of the NIM is approximately 50μm, $\chi^{(2)}$~80pm/V, and peak pump intensity is ~500MW/cm^2. The interaction is consumed entirely near the surface interface, where both fields are more intense. In the absence of absorption, similar conversion efficiencies are possible in bulk PIMs, only by imposing simultaneous phase and group velocity matching. Finally, our calculations show that conversion efficiencies of order 0.2% are also possible, even when the attenuation depth is approximately 5μm, and suggest that similarly efficient higher harmonic generation and parametric amplification may be also achievable in a multi-wave mixing environment under conditions of significant absorption.

Acknowledgments

G.D. acknowledges financial support form the National Research Council. M.C. thanks the Army European Research office in London for partial financial support.

#69149 - $15.00 USD Received 21 March 2006; revised 8 May 2006; accepted 10 May 2006